Designing NHC–copper(I) dipyridylamine complexes for blue light-emitting electrochemical cells

Margaux Elie, Fabien Sguerra, Florent Di Meo, Michael D. Weber, Ronan Marion, Adèle Grimault, Jean-François Lohier, Aurélie Stallivieri, Arnaud Brosseau, Robert B. Pansu, et al.

Designing NHC-Copper(I) Dipyridylamine Complexes for Blue Light-Emitting Electrochemical Cells

Margaux Elie,[‡,†] Fabien Sguerra,[‡,ǁ] Florent Di Meo,[‡,§] Michael D. Weber,[‡,≠] Ronan Marion,[†] Adèle Grimault,[†] Jean-François Lohier,[†] Aurélie Stallivieri,[†] Arnaud Brosseau,[¥] Robert B. Pansu,[¥] Jean-Luc Renaud,[†] Rubén D. Costa,[*,≠] Mathieu Linares,[*,§,♯] Matthieu Hamel,[*,ǁ] Sylvain Gaillard[*,†]

[†] Normandie Univ., LCMT, ENSICAEN, UNICAEN, CNRS, 14000-France.

[ǁ] CEA, LIST, Laboratoire Capteurs et Architectures Électroniques, F-91191 Gif-sur-Yvette Cedex (France).

[§] Division of Theoretical Chemistry, Department of Physics, Chemistry and Biology, Linköping University, SE-581 83 Linköping (Sweden).

[≠] Department of Chemistry and Pharmacy, University of Erlangen-Nuremberg, Egerlandstr. 3, DE-91058 Erlangen (Germany).

[¥] PPSM, CNRS, UMR8531 & Inst. d'Alembert FR3242, ENS Cachan, Paris Saclay University

♯ Swedish e-Science Research Centre (SeRC), Linköping University, SE-581 83 Linköping, Sweden

KEYWORDS: Copper(I) complexes, blue emitters, electroluminescence, light-emitting electrochemical cells, TADF, TD-DFT

ABSTRACT: This study presents the influence of various substituents on the photophysical features of heteroleptic copper(I) complexes bearing both *N*-heterocyclic carbene (NHC) and dipyridylamine (dpa = dipyridylamine skeleton corresponding to ligand **L1**) ligands. The luminescent properties have been compared to our recently reported archetypal blue emitting [Cu(IPr)(dpa)][PF_6] complex. The choice of the substituents on both ligands has been guided to explore the effect of the electron donor/acceptor and "push-pull" on the emission wavelengths and photoluminescence quantum yields. A selection of the best candidates in terms of their photophysical features were applied for developing the first blue light-emitting electrochemical cells (LECs) based on copper(I) complexes. The device analysis suggests that the main concern is the moderate redox stability of the complexes under high applied driving currents, leading to devices with moderate stabilities pointing to a proof-of-concept for further developments. Nevertheless, under low applied driving currents the blue emission is stable, showing performance levels competitive to those reported for blue LECs based on iridium(III) complexes. Overall, this work provides valuable guidelines to tackle the design of enhanced NHC complexes for lighting applications in the near future.

INTRODUCTION

Throughout the last two decades, coordination complexes based on iridium(III), ruthenium(II), platinum(II) and gold(I) have found applications in thin-film lighting technologies based on Organic Light-Emitting Diodes (OLEDs)[1,2] and Light-Emitting Electrochemical Cells (LECs).[3,4] These complexes can theoretically provide devices with external quantum efficiencies close to 100% due to their strong orbital coupling, allowing a high phosphorescence emission. Despite many efforts, commercial OLEDs are very expensive and environmentally unfriendly due to the use of vacuum-processing steps for device fabrication and the lack of efficient recycling protocols of rare elements, respectively. Although it is expected that LECs will be much more cost-efficient than OLEDs due to the simple device architecture and solvent-based production techniques,[5-8] their main disadvantage is the lack of stable and efficient blue-emitting devices and the need of development based on sustainable and cheap coordination complexes, since they entirely constitute the active layer. The search of high-performing compounds with copper as frontrunner is expected to circumvent the above-mentioned roadblocks in the near future.[9-17]

In this context, thermally activated delayed fluorescence (TADF), known as singlet harvesting, has recently emerged as a new paradigm to apply new sustainable emitters that can lead to devices with an internal luminescence efficiency up to 100%.[18,19] Since the pioneering study of McMillin,[20] it is now well-established that copper(I) complexes are archetypal TADF materials. For this reason, the current achievements of TADF lighting devices have recently fueled efforts in developing new copper(I) complexes.[21] This is encompassed with other assets, such as the lower price and higher abundance in the Earth crust than other noble metals. Copper(I) complexes are today emerging as sound alternative for both singlet and triplet harvesters in lighting technologies. Hence, the development of air-, moisture-

and thermally resistant copper(I) complexes with potential modulation of their emission properties[22] is at the forefront of the field. Until now, several architectures of cationic copper(I) complexes have been mainly designed based on tetracoordinated complexes with bidentate dinitrogen or diphosphine ligands.[9,10,23-25] But these cationic copper complexes suffers from the flattening process upon excitation,[26,27] and the dissociation and recombination of ligands in heteroleptic compounds.[28]

Thompson and Yersin,[29-32] and our group[33,34] have recently invested great efforts in developing a new family of mononuclear copper(I) complexes bearing *N*-heterocyclic carbene (NHC)[35] and nitrogen bidentate ligands, which exhibited very promising luminescence properties. The choice of this combination was guided by two main concerns in addition to those above mentioned (*i.e.* the flattening and the dissociation/recombination issues), namely (i) the high stability of the copper(I) complexes provided by the NHC, and (ii) the possibility of the fine tuning of the photoluminescent properties, which are ruled by the easy modulation of the dpa ligand (dpa = dipyridylamine skeleton corresponding to ligand **L1**).

Our first series of NHC copper(I) complexes bearing methyl substituted dpa derivatives as ligands were found to be very efficient blue emitters. To cover a wider range of emission wavelengths, this work provides clear guidelines to modify the electronic properties on both ligands. On one hand, our focus was the variation of substituent on the IPr-based NHC ligand (IPr, 1,3-bis(2,6-di-iso-propylphenyl)imidazole-2-ylidene) (Figure 1). This NHC template appeared to be crucial to obtain the cationic copper(I) complexes of general formula [Cu(NHC)(dpa)][X]. Indeed, in our previous study, we first noticed a CH-π interaction between the hydrogen atoms of the dpa ligand and the aromatic substituent of the NHC which might confer stability to the copper(I) complex.[33] On the other hand, dpa ligands with an electronic diversity were designed (Figure 2). We report herein the synthesis of new cationic copper(I) complexes bearing NHC and dpa derivatives as ligands, their photophysical properties are studied in concert with a full-fledge theoretical characterization, rationalizing the structure/photoluminescence properties relationships, which are key-guidelines for future designs. Finally, as a proof-of-concept, a selection of the best blue-emitting copper(I) complexes has been applied in LECs, showing the first example of a blue LEC based on copper(I) complexes, featuring a similar performance level as the state-of-the-art blue devices based on iridium(III) complexes.

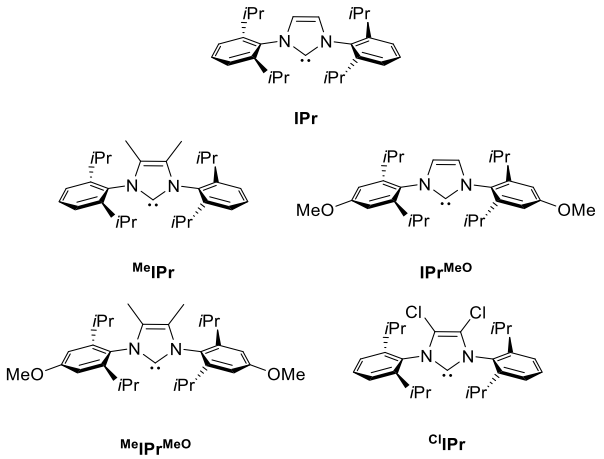

Figure 1. NHC ligands used in this study.

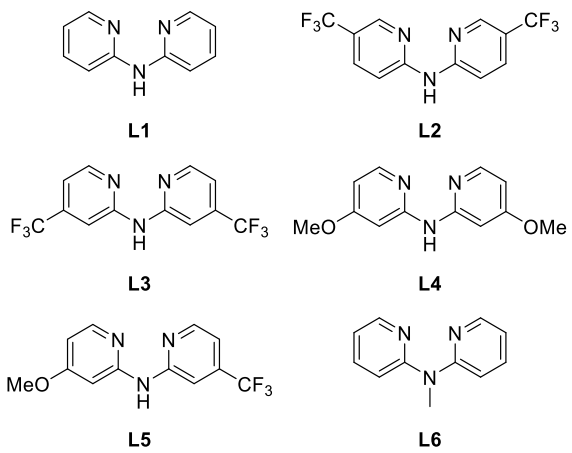

Figure 2. Dpa ligands used in this study.

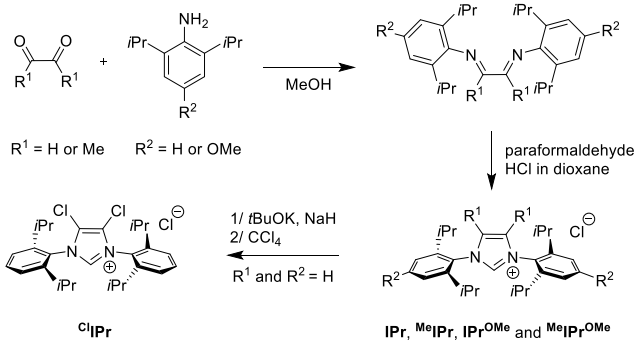

Scheme 1. Synthesis of NHC ligands used in this study.

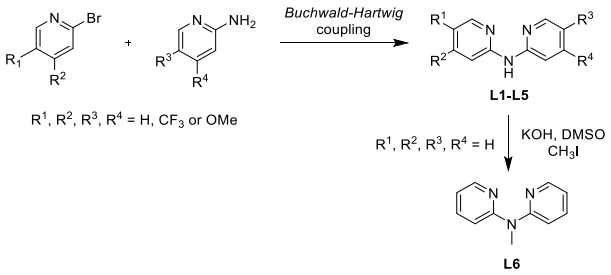

Scheme 2. Synthesis of dpa ligands in this study.

RESULTS AND DISCUSSION

Copper(I) complex synthesis. We first synthesized the ligands shown in Figures 1 and 2. The synthesis of substituted IPr ligands has been conducted following established procedures.[36-37] In detail, *para*-iodination of 2,6-diisopropylaniline by ICl followed by methoxy etherification furnished the 4-methoxy-2,6-diisopropylaniline in 95% overall yield. Then, the imidazolium salts were prepared in a two steps procedure from glyoxal or butan-2,3-dione[36] and the appropriate aniline derivative (Scheme 1). The imidazolium precursor of ^{Cl}IPr was synthesized, following Arduengo's procedure, by reacting the IPr free carbene with CCl_4 (Scheme 1).[37]

Dpa derivatives **L2-L5** were prepared following our previously reported procedure, involving a palladium-catalyzed Buchwald-Hartwig coupling reaction with the appropriate 2-bromopyridines and 2-aminopyridines (Scheme 2).[38] Ligand **L6**

was obtained by alkylation with iodomethane in basic conditions (Scheme 2).[39] With this library of ligands in hand, copper(I) complexes were synthesized in two steps. Firstly, complexes with the formula [CuCl(NHC)] were prepared by reacting imidazolium salts with Cu_2O in refluxing toluene for 12 h.[40] All copper(I) chloride complexes [CuCl(NHC)] **1**-**5** were isolated in moderate to high yields (40 to 94%) as shown in Table 1. Secondly, dpa derivatives were engaged with NHC copper(I) chloride complexes using our previously optimized procedure (Table 2).[33]

The coordination of ligand **L1** with all [CuCl(NHC)] precursors **1**-**5** was successfully achieved with yields ranging between 56 to 90% (Table 1). The coordination of ligands **L1**-**L6** with [CuCl(IPr)] **1** was observed in all cases except with ligand **L2**. In the latter, the starting materials were always recovered. Here, the lower ability of **L2** to coordinate the metal center is ascribed to its electron-deficiency, which might not allow the exchange with the chloride anion. The same explanation might be also put forward with **L3** to explain the low yield (Table 2). Thus, the synthesis of an electronically unsaturated copper(I) complex might be the solution to prepare the corresponding complex. [CuOH(IPr)] (**16**) as precursor of electron deficient copper(I) center was prepared following our previously reported strategy.[33] Addition of a Brønsted acid (*i.e.*, HBF_4) liberated [Cu(IPr)][BF_4], which reacts with ligand **L2**. As the counter-ion can affect the luminescent properties,[41] an additional anion metathesis was carried out to allow a direct comparison of the photophysical properties. Gratifyingly, using this procedure, complex **11** was isolated in 70% yield and the yield of complex **12** was improved up to 77% (Table 2, entries 6 and 7).

Table 1. Synthesis of [CuCl(NHC)] precursors **1**-**5**.[a]

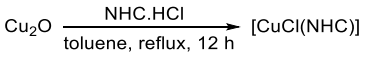

Entry	Complex	Yield (%)[b]
1	[CuCl(IPr)] (**1**)	80
2	[CuCl(^{Me}IPr)] (**2**)	94
3	[CuCl(IPr^{MeO})] (**3**)	82
4	[CuCl(^{Me}IPr^{MeO})] (**4**)	70
5	[CuCl(^{Cl}IPr)] (**5**)	40

a Reaction conditions: Cu_2O (0.65 equiv.), NHC.HCl (1 equiv.), toluene, reflux 24 h. b Isolated yields.

Table 2. Synthesis of [Cu(NHC)(N^N)][X] complexes **6**-**15.**[a]

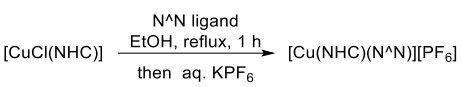

Entry	Complex	Yield (%)[b]
1	[Cu(IPr)(**L1**)][PF_6] (**6**)	72
2	[Cu(^{Me}IPr)(**L1**)][PF_6] (**7**)	90
3	[Cu(IPr^{MeO})(**L1**)][PF_6] (**8**)	86
4	[Cu(^{Me}IPr^{MeO})(**L1**)][PF_6] (**9**)	56
5	[Cu(^{Cl}IPr)(**L1**)][PF_6] (**10**)	82
6	[Cu(IPr)(**L2**)][PF_6] (**11**)	-[c] (70)[d]
7	[Cu(IPr)(**L3**)][PF_6] (**12**)	17 (77)[d]
8	[Cu(IPr)(**L4**)][PF_6] (**13**)	95
9	[Cu(IPr)(**L5**)][PF_6] (**14**)	92
10	[Cu(IPr)(**L6**)][PF_6] (**15**)	75

*a Reaction conditions: [CuCl(NHC)] (1 equiv.), N^N ligand (1.05 equiv.), EtOH, reflux 1 h. b Isolated yields. c Starting material recovered. d [CuOH(IPr)] **16** (1 equiv.), HBF_4 (1 equiv.), toluene, r.t., 12 h then KPF_6, methanol, r.t., 1 h.*

Crystallographic data. As previously reported by Thompson and Yersin groups, conformational feature is a key parameter on the nature of the emitting excited state.[31,32] Therefore, a thorough analysis of crystal structures is required to then assess the influence of substituent pattern on the photophysical property relationship.

Suitable single crystals for XRD analysis (Tables S1-S3) were obtained by slow gas diffusion of pentane into saturated dichloromethane or chloroform solution of copper complexes. Table 3 summarizes the selected bond lengths and angles, as well as the CH···Cg (*i.e.*, distance between the hydrogen atom of the dpa ligand and the centroid of the aromatic ring of the NHC), and the plane angle Θ (*i.e.*, Figure 3 displays this plane angle Θ), which is the angle between the plane of the imidazole ring of the NHC and the plane including the three nitrogen atoms of the dpa ligand as shown in Figures S1-S10 in supporting information (SI) for the measurement.

In general, the Cu-$C_{carbene}$ bond length depends on the electron density in the NHC, reflecting their electron donation ability.[42] As example, bond lengths were 1.9023(17), 1.905(2), 1.909(2), 1.918(4) and 1.927(2) Å in **9**, **8**, **7**, **6** and **10**, respectively (Table 3). In other words, the higher the electron density on NHC, the shorter the Cu-$C_{carbene}$ bond length (Table 3).

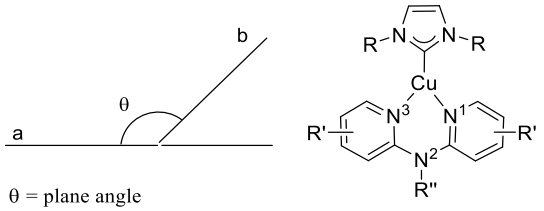

θ = plane angle
a = plane of the imidazole ring of the NHC ligand
b = plane passing by N^1, N^2 and N^3 in the dpa ligand

Figure 3. Definition of the plane angle Θ.

Table 3. Selected bond lengths and angles of copper(I) complexes.

Complex	Cu-$C_{carbene}$ (Å)	Cu···N_{dpa} (Å)	N^1_{dpa}···Cu···N^3_{dpa} (°)	Plane angle Θ (°)[a]	CH···C_g (Å)
[Cu(IPr)(**L1**)][PF_6] (**6**)	1.918(4)	2.040(4) 2.065(4)	90.12(19)	19.948(0.195)	2.56 2.42
[Cu(^{Me}IPr)(**L1**)][PF_6] (**7**)	1.909(2)	2.0477(13)	90.29(8)	43.382(0.075)	2.61

[Cu(IPr^{OMe})(**L1**)][PF_6] (**8**)	1.905(2)	2.027(2) 2.052(2)	91.16(8)	30.349(0.165)	2.38 2.57
[Cu(^{Me}IPr^{OMe})(**L1**)][PF_6] (**9**)	1.9023(17)	2.0316(15) 2.0620(16)	89.48(6)	59.878(0.086)	2.79
[Cu(^{Cl}IPr)(**L1**)][PF_6] (**10**)	1.927(2)	2.0499(14)	90.47(8)	8.336(0.134)	2.32
[Cu(IPr)(**L2**)][PF_6] (**11**)	1.9049(18)	2.0345(17) 2.0566(17)	90.15(6)	49.174(0.082)	2.65
[Cu(IPr)(**L4**)][PF_6] (**13**)	1.911(3)	2.045(3) 2.051(3)	90.31(11)	17.969(0.247)	2.39 2.63
[Cu(IPr)(**L5**)][PF_6] (**14**)	1.9160(15)	2.0327(15) 2.0717(14)	90.27(6)	15.507(0.127)	2.34 2.55
[Cu(IPr)(**L6**)][PF_6] (**15**)	1.911(4)	2.056(4) 2.067(4)	93.68(15)	71.252(0.134)	none

a The plane angle θ is the angle formed by the imidazole ring of the NHC ligand and the plane including the three nitrogen atoms of the dpa ligand calculated using the MPLA instruction (ShelX – Figure 3)

The plane angles Θ have also been measured and appeared to be very different, ranging from 8.336(0.134) to 71.252(0.134)° in complexes **6-15**. Notably, the high value found in **15** had a dramatic impact on the CH-π interactions, usually observed between the aromatic ring of the NHCs and the hydrogen atom of the dpa ligands. These CH-π interactions have been detected in **6-11**, **13** and **14** bearing ligands **L1**, **L2** and **L3-L5** with CH···C_g distance values ranging from 2.32 to 2.79 Å. These features have significant impact on the photoluminescence features of the complexes as carefully described below.

Before discussing the photophysical properties, several aspects have to be pointed out with respect to Thompson and Yersin work.[32] First, unlike the copper(I) complexes reported here, the lowest unoccupied molecular orbital (LUMO) is centered on the NHC ligand in Thompson's and Yersin's works. A detailed molecular orbital (MO) analysis is provided in supplementary information from theoretical calculations. Then, the dipyridylborate is a monoanionic ligand, leading to a neutral complex in Thompson's and Yersin's works, while dpa ligand is a neutral ligand, giving a cationic complex with an outer sphere counterion (PF_6^-). Hence, even if the complex geometries are quite close, the electronic properties might be significantly different.

Photophysical studies. The photophysical properties of compounds are summarized in Table 4 and shown in Figures 4, 5 and S11-S23 in SI. It is important to note that the photophysical characterization of **17-19** from our previous study[33,34] have been added in order to obtain deeper insight into molecular structure/luminescent property relationship. Such complexes bear IPr as NHC and **L7-L9** as dpa ligands (Figure 6).

Figure 4 displays the absorption spectra of **6-15** in solution at room temperature, showing two characteristic bands in the UV region. On one hand, the first intense band at 253 to 266 nm is barely shifted upon varying the nature of the ligands and, in turn, it is assigned to a π-π* ligand centered (LC) transition on the dpa. On the other hand, the lowest-energy bands located at 298-320 nm are marginaly affected by the nature of the NHC ligands but mostly influenced by the dpa subsituents. As such, they are ascribed to dπ-π* metal-to-ligand charge tranfer (MLCT) absorption nature as corroborated by theoretical calculations (*vide infra*).

Regarding the luminescent properties, no emission of the complexes was noted in solution. In contrast, they are, in general, strongly emissive in the solid state. Figure 5 displays the emission spectra that consists of a broad band covering the deep blue-green region from 420 to 550 nm depending on the nature of ligand. In particular, the NHC ligand shows a little effect on the maximum of the emission wavelength of the copper(I) complexes unlike the dpa ligand. For instance, the λ_{em} range was noted around 18 nm for **6-10**, whereas it is much larger (ca. 130 nm) between complexes **6**, **11-15** showing that the fine tuning of the λ_{em} depends more on the electronic properties of the dpa ligand than the one of the NHC ligand (Table 4).

Importantly, the use of symmetrical dpa ligands **L1-L4** and **L8-L9**, bearing electron donor substituents *i.e.*, methoxy (**L4**) and methyl (**L7-L9**) leads to a blue shift in emission, while electron withdrawing groups *i.e.*, trifluoromethyl group (**L2** and **L3**) leads to red-shifted emission spectra, respectively (Table 5). Finally, the replacement of free NH by an alkyl amine (**L6**) resulted in a small blue shift of the emission by 15 nm (Table 4, complex **6** vs. **15**). Overall, these observations are in good agreement with the absorption properties.

Table 4. Photophysical properties of NHC copper(I) complexes **6-19.**

Complex	Absorption[a]	Solid-state emission					
	λ_{max} [nm] (ε [10^4 L.mol^{-1}.cm^{-1}])	λ_{em}[c] [nm]	$\Delta\lambda_{em}$[d] [cm^{-1}]	φ_{em}[c] ± 0.05	τ_{em}[c] [µs]	k_r [10^4 s^{-1}]	k_{nr} [10^4 s^{-1}]
[Cu(IPr)(**L1**)][PF_6] (**6**)	260 (2.31), 315 (1.37)[b]	463	836	0.22	13	1.7	6.0
[Cu(^{Me}IPr)(**L1**)][PF_6] (**7**)	253 (2,37), 306 (1,42)	475	-	0.48	24	2.0	2.2

[Cu(IPr^{MeO})(**L1**)][PF_6] (**8**)	231 (1,66), 253 (1,90), 308 (1,19)	481	-	0.31	29	1.1	2.4
[Cu(^{Me}IPr^{MeO})(**L1**)][PF_6] (**9**)	232 (1,70), 254 (1,91), 307 (1,28)	479	440	0.64	30	2.1	1.2
[Cu(^{Cl}IPr)(**L1**)][PF_6] (**10**)	231 (0,94), 254 (1,71), 272 (1,15), 311 (1,90)	467	-	0.17	10	1.7	8.3
[Cu(IPr)(**L2**)][PF_6] (**11**)	266 (1,77), 313 (1.49)	505	-	0.55	32	1.7	1.4
[Cu(IPr)(**L3**)][PF_6] (**12**)	256 (1,65), 318 (1,08)	≈ 550		< 0.05	5	-	-
[Cu(IPr)(**L4**)][PF_6] (**13**)	253 (1.96), 298 (1,40)	≈ 420	506	< 0.05	20	-	-
[Cu(IPr)(**L5**)][PF_6] (**14**)	232 (2.02), 253 (2.59), 320 (0.78)	521	150	0.20	7	2.9	11.4
[Cu(IPr)(**L6**)][PF_6] (**15**)	230 (0.65), 255 (1.56), 306 (0.88)	473	477	0.36	25	1.4	2.6
[Cu(IPr)(**L7**)][PF_6] (**17**)	259 (2.19), 310 (1.44)[b]	458	337	0.86	44	1.9	0.3
[Cu(IPr)(**L8**)][PF_6] (**18**)	261 (2.32), 316 (1.26)[b]	455	-	0.05	17	0.3	5.6
[Cu(IPr)(**L9**)][PF_6] (**19**)	256 (2.58), 316 (1.28)[b]	460	-	0.43	33	1.3	1.7

a In CH_2Cl_2, concentration 10-4 mol.L-1. b In $CHCl_3$, concentration 10-4 mol.L-1. c room temperature. d 77K.

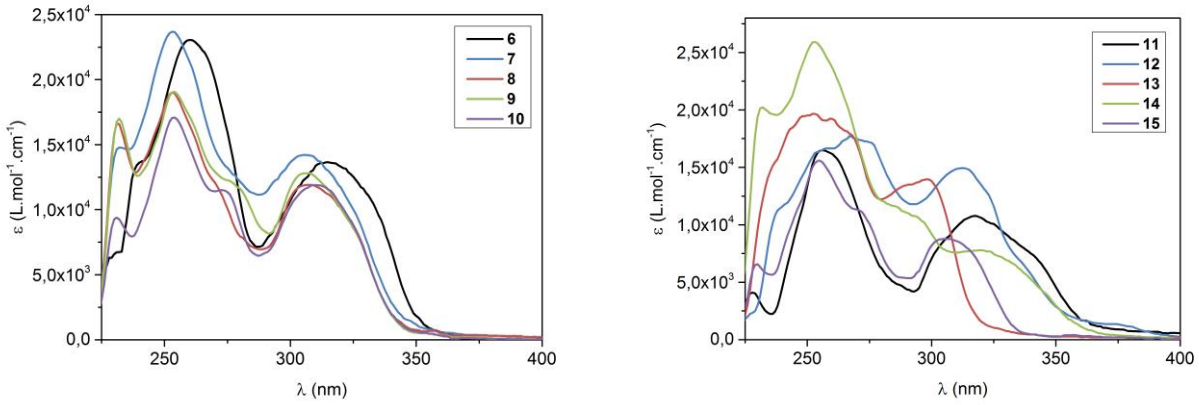

Figure 4. Absorption spectra of complex **6** in $CHCl_3$ and complexes **7**-**15** in CH_2Cl_2.

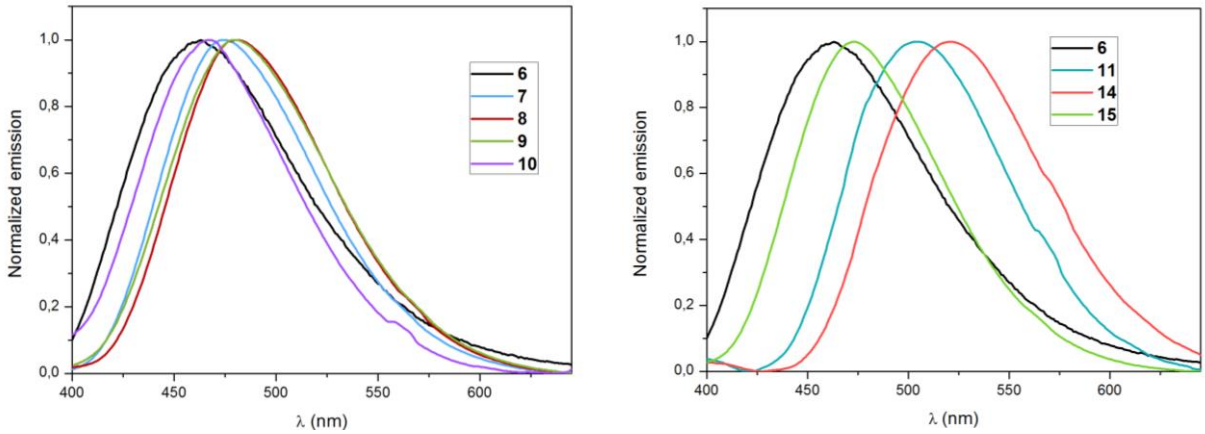

Figure 5. Steady-state emission spectra of **6**-**10**, **11**, **14** and **15** in solid state (powder).

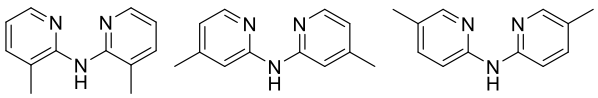

Figure 6. Previously studied dpa ligands.[33,34]

Hence, it is safe to conclude that the photophysical properties of this family are mostly driven by the dpa ligand, which might rule the nature of the excited states as also underlined by theoretical characterizations (*vide infra*).

Next, the photoluminescence quantum yields (φ_{em}) and excited state lifetimes (τ_{em}) at 298 K were measured for all the complexes. The solid-state φ_{em} were found between 0.17 to 0.64 (± 0.05) excepted for complex **12** and **13**, which are very low emissive complexes (Table 4). The τ_{em} are one or two orders of magnitude longer than those assigned to conventional fluorescence with very similar NHC-Cu(I) complexes (Table 4).[32] This

suggests that fluorescence is very unlikely to occur in a part of the emission process. Then, phosphorescence and TADF processes might be considered to rationalize the emission mechanism. As stated in the introduction, TADF or singlet harvesting is a well-known phenomenon in copper(I) complexes. In detail, these materials feature the triplet excited state to be very close in energy to the singlet excited state and, in turn, thermal population of the singlet state is promoted from the triplet state. A qualitative way to determine the existence of this feature is to perform temperature dependence experiments, determining the emission maxima shift at room and 77 K temperatures assays. Upon freezing, a small red-shift in the emission maximum due to the phosphorescence emission is the typical indication of TADF for copper(I) complexes.[18] As a matter of fact, if the nature of the excited state is unchanged upon freezing, a bathochromic shift is noted. To identify this common feature in our complexes, the emission spectrum was recorded at 77 K (Figures S21-S24 in SI). All the studied complexes show the expected red-shifted broad emission of around 150-830 cm^{-1} at 77 K, indicating that the TADF feature is not affected by the pattern substitution of both ligands. This is also corroborated by theoretical calculations (*vide infra*). However, as phosphorescence is characterized by as long decay times as those for the TADF process, a study of the temperature dependence on the τ_{em} was performed.[18] We have selected complexes **6**, as reference, and **17**, presenting the highest φ_{em} in the blue region, and have measured the τ_{em} changes over a temperature range from 295 K to 77 K. As expected, the τ_{em} of **6** and **17** increased from 13 to 45 µs and 44 µs to 81 µs, respectively (Figure 7). The increase by a factor of 2 or 3 is in good agreement with the recent study of Thompson[32] In addition, the decay times of the longer component can be adjusted according to the TADF model used by Steffen and Cisnetti.[43] Here, a fluorescence lifetime of 800 ns and a phosphorescence lifetime of 81 µs was noted for **17**, while **6** shows similar values of 670 ns and 45 µs. The slower decay observed for **17** is due to his higher stabilization energy of 0.09 eV. This supports the presence of TADF process as the emission mechanism in our copper(I) complexes.

Taking into account the latter, we proceed to elucidate qualitative molecular structure/photophysical relationships. The poor luminescent features of **12** and **13** are in good agreement with those previously noted for **18**.[33,34] This seems to be a general trend for symmetrical NHC copper(I) complexes having a 4,4'-substituted dpa ligands (*i.e.*, **L3**, **L4** and **L8**). Finally, this substitution location is of utmost relevance for future design of efficient emitters, as the attachment of bulky groups could be necessary for suppressing the well-known self-quenching issue in solid-state. As such, we have carefully looked at this important aspect. Among others that are studied below, the strong quenching of the emission is typically related to the ligand centered character in the excited state. To circumvent this aspect, the symmetry of the dpa ligand must be broken by asymmetrical substitution or "push-pull" approach (see the substitution pattern in ligand **L3/L4** *vs* **L5** in Figure 2) leading to a more distinct intraligand charge transfer character that should be encompassed by an enhancement of the φ_{em}. A direct comparison of the φ_{em} of **12** and **13** with **15** clearly supports this notion (Table 4). As such, we can safely state that an asymmetrical substitution in the 4,4'-positions should be considered for future design in NHC copper(I) complexes.

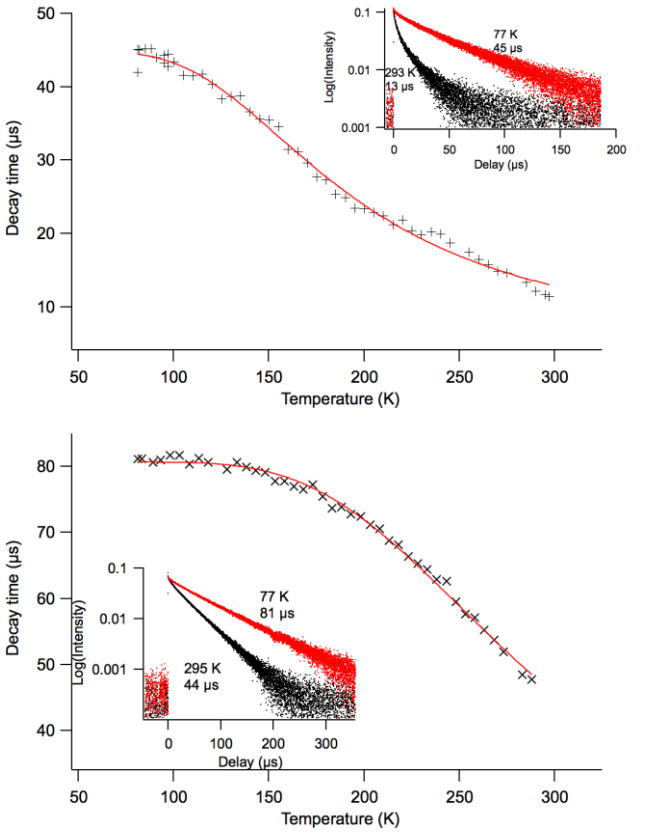

Figure 7. Temperature dependence of the emission lifetime and decay profile at 295 K and 77 K (insets). Top: complex **6**; down: complex **17.** The red line represents the fit of the experimental data.

Another interesting rule can be drawn upon close inspection of the φ_{em} when changing the electronic properties of the NHC ligands, which was considered as "innocent" from analysis of the absorption and emission spectra. In stark contrast, the series of copper(I) complexes bearing the same dpa ligand **L1** (*i.e.*, complexes **6**-**10**), shows that an increase of the σ donation of the NHC goes hand-in-hand with an increase of the φ_{em} *e.g.*, 0.64 *vs.* 0.22 for **9** and **6**, respectively (Figure 8 and Figure S25 in SI).[42] In other words, this interesting molecular structure/luminescent property relationship is also related to the Cu-$C_{carbene}$ bond length, indicating that the shorter the bond length, the higher the φ_{em} (Tables 3 and 4). This shortening of the Cu-$C_{carbene}$ bond length coupled with the CH-π interaction between ligands implies the increase of the plane angle Θ due to electronic repulsions. Finally, another observation has to be pinpointed from the XRD analyses. Indeed, several weak H…F interactions[41,44] between hydrogen atoms of dpa, NHC ligands and the counterion have been detected. Noteworthy, for 4,4'- and 5,5'-substituted dpa ligands NH…F interactions were detected between the hydrogen atom

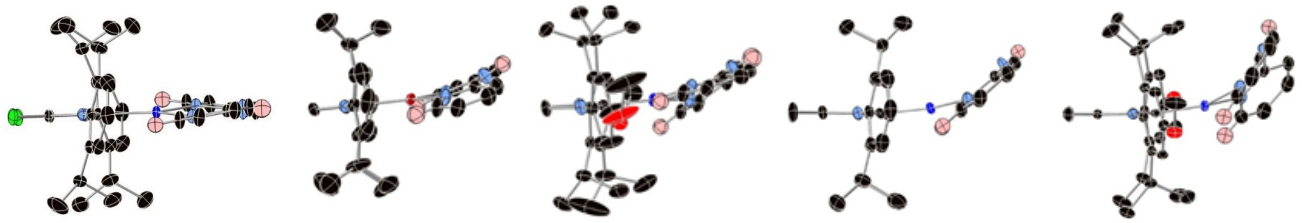

10	**6**	**8**	**7**	**9**
θ = 8.336(0.134)°	θ = 19.948(0.195)°	θ = 30.349(0.165)°	θ = 43.382(0.075)°	θ = 59.878(0.086)°
φ_{em} = 0.17	φ_{em} = 0.22	φ_{em} = 0.31	φ_{em} = 0.48	φ_{em} = 0.64

Figure 8. Comparison of complexes **6**-**10** with the plane angle θ and the ϕ_{em}.

of the bridged nitrogen and a fluorine atom of the PF_6. But, for 3,3'-substituted dpa ligands such as **17**, the NH function is not accessible due to the steric hindrance. The H…F interaction was detected between a hydrogen atom of one methyl substituent of **L7** and PF_6, and led to a symmetry breaking in **17**. Such symmetry breaking was also observed for **15** in which no NH…F interaction is possible due to the *N*-methyl substituent. In this case, an H…F interaction was detected between one fluorine atom of the PF_6 with two hydrogen atoms of one pyridine ring of **L6**. In these two latter cases, the higher symmetry breaking led to an important enhancement of the φ_{em} (Table 4, **6** *vs*. **15** and **18** *vs*. **17**, respectively).[45] Finally, even if the molecular structure/φ_{em} relationship appears difficult to predict, the symmetry breaking in the copper(I) complexes, generated by both the H…F interactions and the plane angle, might be important feature to control the φ_{em}. Concerning the τ_{em} gathered in Table 4, all the complexes show values in the microsecond regime (5 to 44 µs) which are typical for solid-state emission of luminescent copper(I) complexes.[30,31,33,34] Similar to what we noticed for the φ_{em}, the ligand substitution also governs τ_{em}. On one hand, substitution of the NHC ligands does not clearly influence the τ_{em} with the exception of **10** with the chlorine substitution, which lowered both φ_{em} and τ_{em}. This is quite likely related to an internal heavy atom effect as suggested by the non-radiative rate constant (Table 4). On the other hand, by varying the nature and position of the substituents attached to the dpa ligand, τ_{em} from 5-44 µs were noted. Here, since the dpa ligand strongly impacts the emission maxima, it is difficult to provide new conclusions to our previous work.[33,34]

Taking all of the aforementioned results into a broader context, we can highlight two important aspects for the design of NHC copper(I) complexes. Firstly, the substitution of the NHC ligand potentially leads to an increase of the radiative rate constant due to an increase of φ_{em} without affecting emission maxima in the blue region (compare **6**-**10** in Table 4). Secondly, a red-shift of the emission featuring a high φ_{em} can be easily achieved by designing a dpa ligand with a "push-pull" substitution pattern (compare **6** and **14** in Table 4).

Vertical excitations and excited states. Time-dependent DFT calculations of vertical absorption (VA) were performed to unveil the nature of the excited states, supporting the rationalize structure-photoluminescence property relationships (*vide infra*). The presence of copper(I) center provides an efficient singlet-triplet intersystem crossing. Therefore, both singlet-singlet and singlet-triplet transitions were considered (Table 5). The nature of each transition was analyzed *via* Natural Transition Orbitals (NTO) (Table 5 and Figure S27 and S28 in SI). The lower influence of NHC on photophysical properties is theoretically confirmed since no significant differences in vertical excitation energies are obtained between [Cu(IPr)(**L1**)]$^+$, [Cu(^{Me}IPr)(**L1**)]$^+$, [Cu(IPr^{OMe})(**L1**)]$^+$, [Cu(^{Me}IPr^{OMe})(**L1**)]$^+$ and [Cu(^{Cl}IPr)(**L1**)]$^+$. Therefore, the following discussion focuses on the influence of dpa.

Interestingly, $S_0 \rightarrow S_1$ transitions are mainly attributed to dπ-π* MLCT even though the main MO contributions may differ from HOMO or HOMO-1 to LUMO or LUMO+1 (Table 5). This can be easily explained by frontier MO degeneracy. For instance, [Cu(IPr)(**L1**)]$^+$ HOMO and HOMO-1 are spatially and energetically degenerated (ΔE = 0.01 eV) while LUMO and LUMO+1 are quasi-degenerated (ΔE = 0.11 eV). Substituent electronic effects invert HOMO and HOMO-1 or LUMO and LUMO+1 distributions without changing the nature of the transition (Figure S27 in SI). However, according to the substitution pattern, NTO analysis shows an increase of the contribution of intra-ligand (IL) π-π* transition when substitution pattern either "push" from NHC (e.g., [Cu(^{Me}IPr)(**L1**)]$^+$) or "pull" from dpa (e.g., [Cu(IPr)(**L3**)]$^+$). On the contrary, [Cu(IPr)(**L4**)]$^+$ is the only complex, in which substituents are antisynergic to the Cu-dpa MLCT. This complex actually exhibits a specific from the metal center to the NHC moiety.

$S_0 \rightarrow T_1$ transitions are more complicated to rationalize according to substitution pattern, owing to the high density of state between frontier orbitals due to MO degeneracy. Most of them mainly correspond to a mixture of several types, that are, MLCT, IL(π-π*), NHC CT (Table 5 and Figure S28 in SI). CT states are also confirmed by the triplet spin density distribution involving from NHC ligand to dpa through Cu-atom (see Figure S30 in SI). For instance, [Cu(IPr)(**L1**)]$^+$ exhibits a dominant MLCT, while methoxy-substituted NHC complexes are mainly assigned to IL(π–π*) type. A particular attention should be paid to [Cu(IPr)(**L4**)]$^+$ and [Cu(IPr)(**L6**)]$^+$. The presence of electro-donor moieties on the ligand leads to an intraligand CT located on the NHC moiety. Electron-donor moieties push electron density towards NHC as observed in the $S_0 \rightarrow S_1$ transition of [Cu(IPr)(**L4**)]$^+$. However, the former exhibits CT from phenyl ring to the central heterocycle, while the CT in the latter occurs from one phenyl ring to the other.

Theoretical view of the emission properties and TADF. NHC copper(I) complexes have been shown to possibly undergo

Table 5. Vertical Transition Energies, absorption wavelength, main MO description for both first singlet-singlet ($S_0 \rightarrow S_1$) and singlet triplet ($S_0 \rightarrow T_1$) transitions.

	$S_0 \rightarrow S_1$ transition				$S_0 \rightarrow T_1$ transition			
	E (eV)	λ (nm)	Main MO contribution	Type	E (eV)	λ (nm)	Main MO contribution	Type
[Cu(IPr)(**L1**)]$^+$	4.26	291.1	H→L+1 (34%)	MLCT	3.49	355.0	Complex	MLCT
[Cu(^{Me}IPr)(**L1**)]$^+$	4.26	290.7	H-1→L+1 (70%)	MLCT	3.49	355.3	H→L (39%)	MLCT/ IL(π-π*)
[Cu(IPr^{OMe})(**L1**)]$^+$	4.26	291.1	H→L+1 (37%)	MLCT	3.47	357.5	H-1→L (38%)	IL(π-π*)
[Cu(^{Me}IPr^{OMe})(**L1**)]$^+$	4.25	291.6	H→L (64%)	MLCT	3.46	358.6	H-1→L (42%)	IL(π-π*)
[Cu(^{Cl}IPr)(**L1**)]$^+$	4.23	292.9	H-1→L+1 (49%)	MLCT	3.50	354.4	H→L (39%)	MLCT/ IL(π-π*)
[Cu(IPr)(**L2**)]$^+$	3.75	330.7	H→L (88%)	MLCT	3.32	373.0	Complex	IL(π-π*)
[Cu(IPr)(**L3**)]$^+$	4.02	308.7	H→L (94%)	MLCT	3.32	373.8	H-1→L (55%)	MLCT/ IL(π-π*)
[Cu(IPr)(**L4**)]$^+$	4.29	289.4	H→L (50%)	MLCT[a]	3.64	340.4	Complex	NHCCT
[Cu(IPr)(**L5**)]$^+$	4.10	302.2	H→L (79%)	MLCT	3.43	361.5	H-1→L (51%)	MLCT/IL(π-π*)
[Cu(IPr)(**L6**)]$^+$	4.08	303.8	H→L (76%)	MLCT	3.64	340.8	Complex	NHCCT

*a [Cu(IPr)(**L4**)] S0-S1 transition is MLCT to NHC moiety.*

TADF, *i.e.*, back intersystem-crossing (ISC) from T_1 to S_1 states and, if radiative, subsequent fluorescent emission (*vide supra*). Such back ISC phenomenon is thus governed by the singlet-triplet splitting, *i.e.*, the energy gap between S_1 and T_1 states. In NHC copper(I) complexes, the singlet-triplet splitting upper limit has been set to 0.37 eV to thermally populate S_1 state from T_1.[32] It is worth noting that such requirement is strongly related to a sufficient HOMO-LUMO spatial separation.[18,46,47] While the HOMO-LUMO separation can be theoretically assessed from conventional GS DFT-calculations, ΔE^{ST} has to be calculated from adiabatic excitation energies. Thereby, for each complex, the first excited triplet state T_1 geometries were optimized through optimized spin-relaxed open shell calculations. All calculations were carried out at the ωB97X-D/6-31+G(d,p)/SDD level of theory.

The occurrence of TADF is supported by calculations since all calculated ΔE^{ST} are lower than 0.37 eV (Table 6). However, back ISC may occur with more or less significance for all complexes since calculated ΔE^{ST} range from 0.12-0.37 eV. Besides singlet-triplet splitting, these compounds also met the HOMO and LUMO spatial separation. As TADF process have been experimentally demonstrated for complex **6** (*vide infra*), it is reasonable to consider that the theoretical value of 0.35 eV found for the ΔE^{ST} of complex **6** is representative for the presence of TADF in the emission mechanism and all of our complexes should be considered as singlet harvesters. Furthermore, such value is in agreement with the TADF threshold (0.37 eV or 3000 cm^{-1}) defined for similar systems.[32]

In agreement with previous works,[31,32] the conformation deformation upon the different S_0, T_1 and S_1 states has been investigated to rationalized emission process. Selected geometrical data and RMSDs are reported in the SI as well as XYZ coordinates.[48] Significant geometrical deformations were observed for T_1 and S_1 optimized geometries with respect to S_0 ones leading to: (i) a rotation of dpa ligand with respect to $N_{carbene}$-Cu(I) bond axis and (ii) a folding of dpa ligand associated to an increase of NHC-dpa plane angles. The former deformation has been shown to play an important role in TADF processes. The lower the ligand rotation, the higher the TADF for a given structure. For example, the $N_{imidazole}$-$C_{carbene}$…Cu-N_{dpa} dihedral rotations of [Cu(IPr)(**L2**)]$^+$ and [Cu(IPr)(**L4**)]$^+$ are ca. -29° and -7° while ΔE^{ST} are 0.36 and 0.12 eV, respectively. Leitl and co-workers have shown that such rotation leads to a delocalization of HOMO to the NHC ligand leading to a HOMO-LUMO orthogonal separation that decreases the coupling between them.[32] However, such a large (small) rotation is not necessarily associated to a large (small) ΔE^{ST}. Therefore, the dihedral rotation is not sufficient to rationalize the importance of TADF. Furthermore, the dihedral angle rotation should also be considered according to the deformation with respect to S_0 state (namely rotational deviation) picturing the excited state molecular flexibility. The lower the molecular flexibility, the lower the non-radiative decay of exciton, the more likely the radiative emission.[18] Strong conformational change between S_1 and T_1 leads to an increase of ΔE^{ST} since back ISC would be energetically less favored. Sterically congested molecules exhibit small deformation between S_1 and T_1 structures lowering ΔE^{ST}. For instance, [Cu(IPr)(**L6**)]$^+$ exhibit the most congested Cu-center by the presence of methyl group on central dpa *N*-atom; it exhibits the lowest geometrical deviation between S_1 and T_1 states while rotational deviation is relatively high (Table S6 in SI). Therefore, [Cu(IPr)(**L6**)]$^+$ exhibits a ΔE^{ST} = 0.24 eV, being moderately lower than the [Cu(IPr)(**L1**)]$^+$ reference (ΔE^{ST} = 0.35 eV). For [Cu(IPr)(**L4**)]$^+$, the S_0 dihedral rotation is small in conjunction with a slight conformational S_1-T_1 deformation (RMSD(S_1/T_1) = 0.17) as well as the smallest singlet-triplet splitting (ΔE^{ST} = 0.12 eV). Finally, the $C_{carbene}$-Cu(I) bond distance is the last conformational parameter that should be investigated upon light excitation. The MLCT nature described in vertical excitation is confirmed since $C_{carbene}$-Cu(I) is systematically increased for all complexes except [Cu(IPr)(**L4**)]$^+$ as well as asymmetrical Cu-N_{dpa} bond shortening (Table S6 in SI). Interestingly, $C_{carbene}$-Cu bond is almost not changed in both S_1 and T_1 states with respect to S_0 in [Cu(IPr)(**L4**)]$^+$. This confirms (i) the absence of MLCT nature in this complex and (ii) that small conformational changes in three states are strongly correlated to singlet-triplet splitting decrease. These conformational changes are particularly important since they also capture the dependence of singlet-triplet splitting on MLCT electron-hole recombination: the higher the electron-hole recombination distance, the lower the singlet-triplet splitting.[46,47]

Table 6. Experimental emission energies, theoretical $S_1 \rightarrow S_0$ and $T_1 \rightarrow S_0$ emission energies and calculated singlet-triplet splitting.

Complex	Exp (eV)	$S_1 \rightarrow S_0$ (eV)	$T_1 \rightarrow S_0$ (eV)	ΔE^{ST} (eV)
$[Cu(IPr)(\mathbf{L1})]^+$	2.54	3.00	2.59	0.35
$[Cu(^{Me}IPr)(\mathbf{L1})]^+$	2.61	2.98	2.75	0.24
$[Cu(IPr^{OMe})(\mathbf{L1})]^+$	2.58	2.98	2.57	0.36
$[Cu(^{Me}IPr^{OMe})(\mathbf{L1})]^+$	2.59	2.95	2.59	0.35
$[Cu(^{Cl}IPr)(\mathbf{L1})]^+$	2.65	3.04	2.79	0.29
$[Cu(IPr)(\mathbf{L2})]^+$	2.46	2.75	2.35	0.36
$[Cu(IPr)(\mathbf{L3})]^+$	2.25	2.68	2.27	0.37
$[Cu(IPr)(\mathbf{L4})]^+$	2.95	3.25	3.05	0.12
$[Cu(IPr)(\mathbf{L5})]^+$	2.38	2.61	2.21	0.36
$[Cu(IPr)(\mathbf{L6})]^+$	2.62	2.97	2.74	0.24

Beside conformational changes, a particular attention has been paid to the nature of both $S_1 \rightarrow S_0$ and $T_1 \rightarrow S_0$ transitions regarding to MLCT. Such properties may be pictured by the NTO analysis of $S_1 \rightarrow S_0$ and $T_1 \rightarrow S_0$ transitions from TD-DFT calculations on S_1 and T_1 geometries (Figure S31 and S32 in SI). Except for $[Cu(IPr)(\mathbf{L4})]^+$, T_1-S_0 transitions mainly exhibit backligand to metal CT from dpa to the trigonal Cu(I) center involving π^* and mixture of d- and n-orbitals for T_1 and S_0, respectively (Figure S32 in SI). $S_1 \rightarrow S_0$ NTO analysis provides the same hints except that π^* is significantly more localized on one pyridine ring of dpa.

Regarding emission energies reported in Table 6, differences between experiments and theory can be explained by the absence of counterions in the calculations. Thereby, the following discussion is based on the electronic features. Trends between complexes are well-reproduced considering that room-temperature emissions are attributed to a mixture of $T_1 \rightarrow S_0$ and $S_1 \rightarrow S_0$ transitions. For most of complexes, the relatively high values of ΔE^{ST} show that back ISC occurs as a minor event; which suggests radiative $T_1 \rightarrow S_0$ transition as the driven emission process at room temperature. On one hand, this is supported by theoretical calculations in which the relation-structure property is well-reproduced by T_1-S_0 transition calculations. On the other hand, differences of emission energies with respect to $[Cu(IPr)(\mathbf{L1})]^+$ are not only explained by electronic effects of substitution pattern but also by the probability of back ISC pictures. Indeed, experiments provide a systematic blue-shift of emission energies for complexes exhibiting a lower singlet-triplet splitting (Table 6). The lower the ΔE^{ST}, the higher the $S_1 \rightarrow S_0$ emission, which is obviously blue-shifted with respect to $T_1 \rightarrow S_0$. Interestingly, while absorption properties has been shown to not be strongly affected when the NHC ligand was modified, the blue-shift of $[Cu(^{Me}IPr)(\mathbf{L1})]^+$ with respect to $[Cu(IPr)(\mathbf{L1})]^+$ is partially attributed to the slightly higher occurrence of TADF process. A relatively good correlation between emission time and TADF process is also observed. For most of complexes, a lower ΔE^{ST} is often associated to a lower emission time suggesting a higher occurrence of TADF along emission (Tables 4 and 6).

LEC fabrication and analysis. A simple two-layer LEC was prepared to investigate the electroluminescent properties of the NHC copper(I) complexes. Prior to the deposition of the active layer, a thin layer (100 nm) of polyethylene dioxythiophene:polystyrene sulfonic acid (PEDOT:PSS) was doctor-bladed to ensure the device reproducibility. The compounds **9**, **14**, and **17** were tested, as they show the best photoluminescence features of the two extremes, that is, the higher-energy (**9** and **17**) and lower-energy (**14**) emission wavelengths still featuring high φ_{em} (*vide supra)*. Owing to the simple molecular structure, complex **6** was also considered for reference purposes. In detail, an active layer of around 100 nm was prepared by means of doctor-blading in a two-step process out of THF solution, showing homogenous layers with a surface roughness of <5%. Immediately, the thin films were transferred into an inert atmosphere glove-box system, in which aluminum was deposited as the top electrode contact. The devices were analyzed using current-voltage-luminance (IVL) and assays with a dV/dt scan rate of 0.20 V/s and were driven using a pulsed current scheme based on a block-wave at 1000 Hz and a duty cycle of 50 %. Notably, this driving mode has led to the best performing LECs in terms of a stable performance and ultra-fast turn-on times.[3,4] Details concerning the device preparation and analysis can be found in the experimental section.

As a first approach, IVL assays were performed (Figure 9 and Figure S43 in SI), showing a general low turn-on injection voltage (*i.e.*, voltage value at which current injection starts) and relatively low current density values even at high voltages. The latter are usual in LECs due to the presence of the mobile anions, which, upon applying voltage, efficiently assist the charge injection process at the electrode interfaces. As the most interesting example, devices prepared with **6** and **17** show maxima luminance levels of around 56 and 310 cd/m^2, respectively. The latter are associated to a broad shape electroluminescence (EL) spectrum centered at 490-500 nm with Commission Internationale de l'Eclairage 1931 (CIE) coordinates of approx. x = 0.23/ y = 0.28, that is, the first example of a blue LEC based on copper(I) complexes (Figure 9). It is important to note, that the device is not stable under repetitive IVL sweeps from 0 to 11 V, showing a drop in luminance with a slightly red-shifted EL spectrum (Figure 9). This suggests that over oxidation/reduction processes are slightly degrading the copper(I) complexes,[33] while the strong applied field might be responsible of the EL shift. Other aspects like degradation of the complex prior device fabrication cannot be ruled out, as they show a moderate stability in THF (Figure S44 and S45). This aspect is carefully discussed below. Nevertheless, this behavior seems to be general, since similar results were obtained for the green-emitting copper(I) complex, *i.e.* **14**, showing luminance values of 2.7 cd/m^2 and an EL spectrum centered at 555 nm with a red-shift of 9 nm upon repetitive IVL (Figure S42 in SI).

Next, the devices with **6**, **9**, and **17** were driven at different applied currents as summarized in Table 7. Since all the devices show the same device behavior over time, a representative example based on complex **17** is shown in Figure 10, while Figure S46 in SI shows the device performance of the other complexes and Table 7 summarizes the most relevant figures-of-merit. Under these conditions, all devices showed a typical LEC behavior as derived from the average voltage profile. In detail, the applied voltage rapidly drops due to the migration of the mobile anions that enhance the injection process, reaching a short-time plateau until it starts to slowly increase when the device starts to degrade. As recently demonstrated by Gao *et al.*,[49] this is attributed to the formation of pin-holes and/or black spots associated to the degradation of the emitting material by means of ei-

ther a reaction with the cathode over time under storage conditions or an over oxidation/reduction process under device operation conditions.

During the first two stages of the device lifetime, an instantaneous luminance was detected (*i.e.*, the turn-on time defined as the time to start to detect luminance is in the ms regime) and was increased until reaching its maximum after 30 s for all the devices, except the lowest galvanostatic driven LEC, in which the brightness peaks after 10 min. Unfortunately, once the maximum is achieved the luminance exponentially decays, showing lifetimes of 3 to 15 min (Table 7). Here, the luminance decay goes hand-in-hand with the increase of the average applied voltage, suggesting that the main reason could be the degradation of the copper(I) complex due to uncontrolled over oxidation/reduction processes. Besides the low electrochemical redox stability of the complex,[33] other aspects that also pinpoint to this reason are i) the red-shift of the EL spectra over time, indicating that the emitter is degrading, and ii) the lack of EL emission when a post-mortem device is heated at 90 ºC for 30 min to remove the formed doped layers that typically reactivates the device.[50] However, if the applied currents are kept low, a small shift of the EL spectrum was noted, ensuring that the blue color is kept until the device is dead (Figure 10).

For a deeper understanding about the copper(I) complex stability issue in LECs, the aging of **17** in THF was investigated. The aged solutions (10 min, 1 h, 20 h and 40 h) were doctor-bladed on quartz substrates. Then, the emission, the τ_{em}, and the relative φ_{em} of all the thin films were measured at 295 K. Both λ_{em} and τ_{em} remain unchanged for all samples (*i.e.*, the same wavelength maximum at 458 nm and the same τ_{em} of 44 µs). Nevertheless, concerning φ_{em}, only a loss of 4% on the relative φ_{em} after 1 h was noted, while it increases up to 15% after 20 h and to 63% after 40 h. This result indicates that **17** might be stable in THF during the device production time, but the absorption features over time show the formation of a new band in the region of 350-450 nm that are attributed to the oxidation of the complex under ambient conditions (Figure S44 and S45). The presence of the latter did not dramatically affect the emission features of the complexes for a short aging times (1-10 min). Since the LECs were prepared with fresh copper(I) complex solutions that are used after 1-3 min and then the films are directly transferred to an inert atmosphere, we assume that the short lifetime of the devices is primarily attributed to a redox issue when high voltages are applied (*vide supra*), but the impact of the new species on the electronic behavior of the devices cannot be ruled out. Indeed, further efforts are currently in process to understand the degradation mechanism in order to propose better copper(I) complexes for LEC devices in the future.

Besides the latter, our blue LECs show figures-of-merit that are surprisingly comparable to those achieved for blue-emitting LECs based on iridium(III) complexes.[51-63] Efficacy values of LECs with **6** and **9** are low due to the required high current densities to obtain a comparable functional device in terms of, for example, luminance levels. Here, these devices consume more power and consequently suffer the loss of their lifetime (Figure S46 in SI). Here, we must point out that we are working on a further optimization of the devices in terms of charge transport features and suppression of aggregates that act as quenchers.

Table 7. Device figures-of-merit under different applied currents.

Complex	Average current density [mA/cm²]	Luminance [cd/m²]	Efficacy [cd/A]	$t_{1/2}$ [min]	λ_{max} [nm] and CIE
6	166.4	5.9	0.004	1.3	495 0.24/0.29
9	166.5	10	0.006	1.2	493 0.23/0.29
17	9.97	22.2	0.22	16.5	497 0.23/0.28
17	16.65	48.2	0.29	2.7	
17	33.2	80.3	0.24	3.0	

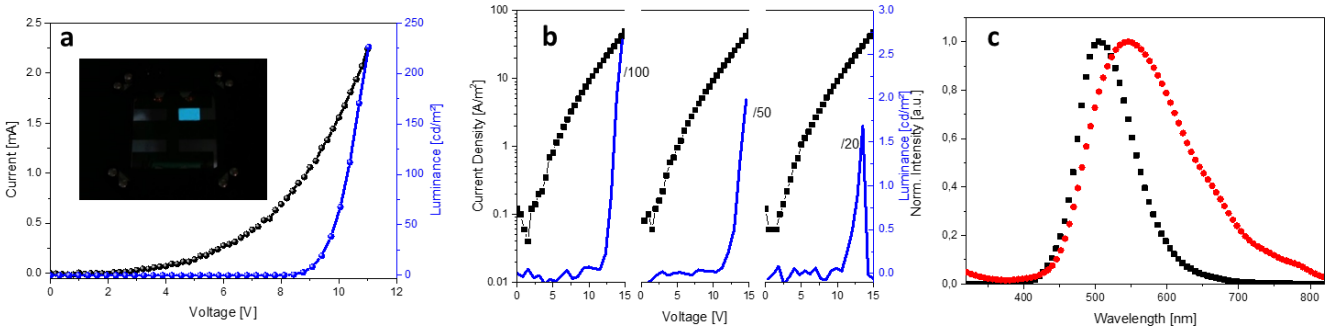

Figure 9. a) IVL-scans of devices with **17** at a scan rate of dV/dt = 0.2 V/s in a voltage range of 0-11 V. Inset picture shows the blue LEC during the first IVL cycle. b) Repetitive IVL assays at a scan rate of dV/dt = 0.2 V/s in a voltage range of 0-15 V. c) EL shift from the initial device response (black squares) to the last recorded spectra (red circles) in the first and third IVL scans, respectively.

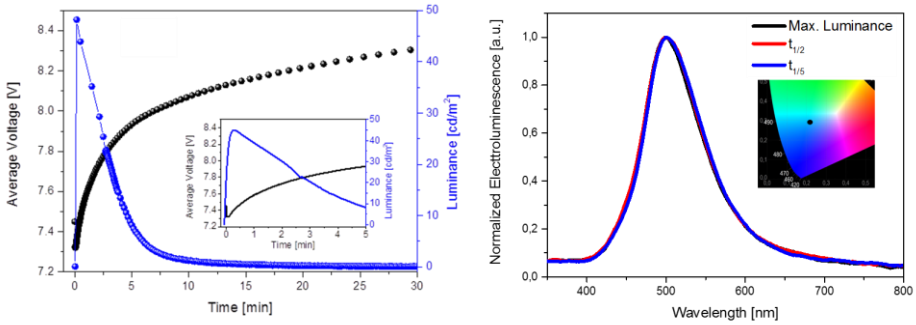

Figure 10. Lifetime measurement in galvanostatic pulsed driving mode at 2.5 mA of a device containing **17**. Inset features the initial voltage response and displaying the typical LEC-behavior (left). Changes of the EL spectra under operation condition over time with the CIE coordinated as an inset (right).

CONCLUSION

Several new copper(I) complexes with the general formula [Cu(NHC)(dpa)][PF_6] have been synthesized to establish for the first time clear molecular structure/luminescent properties relationship guidelines for future designs. The latter are derived from a comprehensive photophysical, and theoretical study.

In detail, the electronic properties of dpa ligands clearly control the emission maxima. Indeed, electron donor substituents lead to blue-shift, whereas electron withdrawing groups lead to a red-shift for the emission. The combination of both in a "push-pull" scheme increases the CT character of the excited state, enhancing the luminescent features. In addition, the high φ_{em} observed in some complexes seem to find an explanation by the symmetry breaking generated by both the plane angle Θ and the different H...F interactions between the dpa ligand and the counterion. Then, the presence of the TADF process as a part of the emission property has been experimentally demonstrated for this copper(I) complex family and was additionally supported by TD-DFT calculations.

As a proof of concept, four of the most interesting complexes were applied in LECs. As expected, devices based on the copper(I) complex with the highest φ_{em} (*i.e.*, **17**) feature an interesting blue-emitting electroluminescent response that is stable at low applied driving currents with comparable luminance and efficacy to blue LECs based on iridium(III) complexes. Nevertheless, it is important to point out that this type of complexes slowly degrades in solution under ambient conditions and shows an intrinsic redox stability.[33] Both aspects need to be taken into account for the design of both future complexes and device fabrication protocols. Other aspects like film morphology, degradation of the complexes prior and after film formation, as well as degradation under storage conditions after depositing the cathode cannot be ruled out at this stage. Ongoing work in our laboratories is currently focused on understanding the impact of the above-mentioned aspects on the device performance. Overall, this work provides valuable guidelines to tackle the design of enhanced NHC complexes for lighting applications in the near future.

EXPERIMENTAL SECTION

General characterization techniques and materials: Solvent were purchased from Carlo Erba and degassed prior to use by bubbling argon gas directly in the solvent. NMR spectra were recorded on a 400 MHz and 500 MHz Bruker spectrometers. Proton (^{1}H) NMR information is given in the following format: multiplicity (s, singlet; d, doublet; t, triplet; q, quartet; qui, quintet; sept, septet; m, multiplet), coupling constant(s) (*J*) in Hertz (Hz), number of protons. The prefix *app* is occasionally applied when the true signal multiplicity was unresolved and br indicates the signal in question broadened. Carbon (^{13}C) NMR spectra are reported in ppm (δ) relative to residual $CDCl_3$ (δ 77.0) unless otherwise noted. HRMS analyses were performed by LCMT analytical services. NMR solvent was passed through a pad of basic alumina before use. UV-visible spectra were measured at room temperature in dichloromethane (chloroform for complexes **17-19**) on a Jenway 6715 UV/Vis spectrometer, wavelengths are given in nm and extinction coefficients ε are presented in $L.mol^{-1}.cm^{-1}$. Steady-state emission spectra and emission lifetime were recorded with solid state on a Horiba Jobin Yvon Fluoromax-4P spectrofluorometer. For measuring absolute solid-state emission quantum yield, a Horiba Jobin Yvon integrating sphere F-3018 was equipped to the Fluoromax-4P spectrofluorometer.

General procedures for the synthesis of [Cu(NHC)(dpa)][PF_6] complexes.[33] (Procedure 1) In a flame-dried Schlenk tube under argon atmosphere, [CuCl(NHC)] complex (1 equiv.) and dpa ligand (1.05 equiv.) were dissolved in degassed absolute ethanol and heated to reflux for one hour. After cooling to room temperature, a saturated aqueous solution of KPF_6 was added, affording a white precipitate. The solid was washed with water and dried in vacuum. (Procedure 2) In a flamed-dried Schlenk tube under argon atmosphere, [CuOH(IPr)] complex (1 equiv.) and dpa ligand (1 equiv.) were dissolved in dry degassed toluene. $HBF_4{\cdot}Et_2O$ (1 equiv.) was added dropwise and the reaction mixture was stirred overnight at room temperature. Pentane was added, affording a precipitate which was collected on a frit, washed with pentane and dried in vacuum. Then, in a round bottom flask, the obtained [Cu(IPr)(dpa)][BF_4] complex and KPF_6 (5 equiv.) were dissolved in MeOH, the mixture was stirred for 1 hour at room temperature. The mixture was then concentrated to dryness, the complex was dissolved in DCM, filtered through a pad of celite® and concentrated again, leading to the [Cu(IPr)(dpa)][PF_6] complex as a powder.

X-ray crystallography. Crystallographic data sets were collected from single crystal samples. Collections were performed

using a Bruker Kappa APEXII CCD diffractometer. The initial unit cell parameters were determined by a least-squares fit of the angular setting of strong reflections, collected by a 6.0° scan in 12 frames over three different parts of the reciprocal space (36 frames total). Cell refinement and data reduction were performed with SAINT (Bruker AXS). Absorption correction was done by multiscan methods using SADABS-2012/1 (Bruker AXS). The structure was solved by direct methods and refined using either SHELXL-97 or SHELXL-2013 (Sheldrick). All non-H atoms were refined by full-matrix least-squares with anisotropic displacement parameters while hydrogen atoms were placed in idealized positions. Crystal data and details of the data collection and refinement are summarized in Table S1, S2 and S3. CCDC numbers (1402282-1402289) contain the supplementary crystallographic data for this article. These data can be obtained free of charge from the Cambridge Crystallographic Data Centre *via* www.ccdc.cam.ac.uk/data_request/cif.

Computational details. Calculations have been performed with the Gaussian 09 package.[64] Ground states geometries have been optimized using the ωB97XD functional,[65] which is a long-range corrected functional and has been parameterized to take into account dispersive forces. The use of dispersion-corrected functional is mandatory to properly non-covalent interactions such as the CH-π observed in our complexes. The effective core potential SDD was used for the copper atom and the 6-31+G(d,p) basis set for carbon, nitrogen and hydrogen. Frequency calculations have been performed to ensure that the obtained geometries were in the global minimum of the potential energy surface. TD-DFT calculations were performed at the same level of theory. Inorganic complexes are expected to undergo excited state charge transfer (*e.g.*, MLCT, LC-CT).[66] Classical hybrid functionals (*e.g.*, B3LYP) are well known to fail at describing such event. This can be overcome by using range-separated formalism as in ωB97XD. Over the past year, this has shown reliable results with excited state charge transfer in organic[67] and inorganic systems.[68]

The S_0, S_1 and T_1 densities for each studied complexes (Figures S27-S28 and S30-S31 in SI) were done via natural transition orbitals (NTO). This successful approach aims at plotting the global MO distributions for both GS and ES in which all MOs involved in the electronic transition of interest are weighted by the CI coefficients.[69] Visualization has been performed with the VMD program.[70]

Device preparation and analysis. Double layer LECs were fabricated as follows. ITO coated glass plates were patterned by conventional photolithography (Naranjo Substrates). The substrates were cleaned by using sequential ultrasonic baths, namely in water-soap, water, ethanol, and propan-2-ol solvents. After drying, the substrates were placed in a UV–ozone cleaner (Jetlight 42-220) for 8 min. An 100 nm layer of PEDOT:PSS was doctor-bladed onto the ITO-glass substrate to increase the device preparation yield (Zehtner ZAA 2300 using a ZUA 2000 blade with a 400 µm substrate distance and a speed of 10 mm/s). The luminescent layer was entirely prepared with copper(I) complexes using a concentration of 20 mg/mL in THF. The active layer was deposited by means of doctor blading technique (600 µm substrate distance and a speed of 20 mm/s) reaching a thickness of 90-100 nm. These conditions resulted in homogenous thin films with a roughness less than 5 %, having no apparent optical defects. The latter was determined using the profilometer DektakxT from Bruker. Once the active layer was deposited, the samples were transferred into an inert atmosphere glovebox (<0.1 ppm O_2 and H_2O, Innovative Technology). Aluminum cathode electrode (75 nm) was thermally evaporated using a shadow mask under high vacuum (<1·10–6 mbar) using an Angstrom Covap evaporator integrated into the inert atmosphere glovebox. Time dependence of luminance, voltage, and current was measured by applying constant and/or pulsed voltage and current by monitoring the desired parameters simultaneously by using Avantes spectrophotometer (Avaspec-ULS2048L-USB2) in conjunction with a calibrated integrated sphere Avasphere 30-Irrad and Botest OLT OLED Lifetime-Test System. Electroluminescence spectra were recorded using the above mentioned spectrophotometer.

ASSOCIATED CONTENT

Supporting Information. X-ray crystallographic data for complexes **6**, **8**-**10**, and **12**-**14** in CIF format. Additional synthesis procedure for complexes **6**-**14** and ligands ^{Me}IPr, IPr^{OMe}, ^{Me}IPr^{OMe}, ^{Cl}IPr and **L1**-**L6**; Crystallographic and structure refinement data; Absorption and emission spectra of copper complexes, additional DFT studies. This material is available free of charge via the Internet at http://pubs.acs.org.

AUTHOR INFORMATION

Corresponding Author

* E-mail: sylvain.gaillard@ensicaen.fr. Laboratoire de Chimie Moléculaire et Thioroganique, UMR CNRS 6507, FR3038, Ensicaen, 6 Bd du Maréchal Juin, 14050 Caen, France.
* E-mail: matthieu.hamel@cea.fr
* E-mail: mathieu@ifm.liu.se
* E-mail: ruben.costa@fau.de

Author Contributions

The manuscript was written through contributions of all authors. All authors have given approval to the final version of the manuscript. ‡These authors contributed equally.

Notes

The authors declare no competing financial interest.

ACKNOWLEDGMENT

This work was supported by the "Ministère de la Recherche et des Nouvelles Technologies", CNRS (Centre National de la Recherche Scientifique) and the LABEX SynOrg (ANR-11-LABX-0029). We thank the “Agence Nationale de la Recherche”, within the CSOSG program (ANR-12-SECU-0002-02), the ANR program (ANR-15-CE39-0006) and the “Région Basse-Normandie” for their funding (R.M., F.S., M.E. and A.S.). M.L. acknowledges SeRC (Swedish e-Science Research Center) for funding. F.D.M. thanks the Swedish Research Council (Grant No. 621-2014-4646). F.D.M. and M.L. acknowledge SNIC (Swedish National Infrastructure for Computing) for providing computer resources (snic001-12-192). RDC and MDW acknowledge the support by the ‘Fonds der Chemischen Industrie’ (FCI) in the Liebig grant framework and by the EAM Starting Grant of the Cluster of Excellence ‘Engineering of Advanced Materials’ (EAM) promoted by the German Research Foundation (DFG) within the framework of its ‘Excellence Initiative’. F.D.M. and M.L. are grateful to Prof. J.C. Sancho-Garcìa for his generous support.

ABBREVIATIONS

TADF thermally activated delayed fluorescence, NHC, N-Heterocyclic Carbene, dpa dipyridylamine, LEC Light emitting electrochemical cells.

REFERENCES

[1] Yersin, H. Highly Efficient OLEDs with Phosphorescent Materials, Wiley-VCH Verlag GmbH & Co. KGaA: Weinheim, **2008**.

[2] Yersin, H.; Rausch, A. F.; Czerwieniec, R.; Hofbeck, T.; Fischer, T. The Triplet State of Organo-transition Metal Compounds. Triplet Harvesting and Singlet Harvesting for Efficient OLEDs *Coord. Chem. Rev.* **2011**, *255*, 2622-2652.

[3] Costa, R. D.; Ortí, E.; Bolink, H. J.; Monti, F.; Accorsi, G.; Armaroli, N. Luminescent Ionic Transition-Metal Complexes for Light-emitting Electrochemical Cells *Angew. Chem. Int. Ed.*, **2012**, *51*, 8178-8211 and references therein

[4] Meier, S. B.; Tordera, D.; Pertegás, A.; Roldán-Carmona, C.; Ortí, E.; Bolink, H. J. Light-emitting Electrochemical Cells: Recent Progress and Future Prospects *Mater. Today* **2014**, *17*, 217-223.

[5] Zhang, Z.; Guo, K.; Li, Y.; Li, X.; Guan, G.; Li, H.; Luo, Y.; Zhao, F.; Zhang, Q.; Wei, B.; Pei, Q.; Peng, H. A Colour-tunable, Weavable Fibre-shaped Polymer Light-emitting Electrochemical Cell *Nature Photonics* **2015**, *9*, 233-238.

[6] Sandström, A.; Asadpoordarvish, A.; Enevold, J.; Edman, L. Spraying Light: Ambient-air Fabrication of Large-area Emissive Devices on Complex-shaped Surfaces *Adv. Mater.* **2014**, *26*, 4975-4980.

[7] Asadpoordarvish, A.; Sandström, A.; Bollström, R.; Toivakka, M.; Österbacka, R.; Edman, L. Light-Emitting Paper *Adv. Func. Mater.* **2015**, *25*, 3238-3245.

[8] Aygüler, M. F.; Weber, M. D.; Puscher, B. M. D.; Medina, D. D.; Docampo, P.; Costa, R. D. Light-emitting Electrochemical Cells Based on Hybrid Lead Halide Perovskite Nanoparticles *J. Chem. Phys. C* **2015**, *119*, 12047-12054.

[9] Armaroli, N.; Accorsi, G.; Holler, M.; Moudam, O.; Nierengaren, J.-F.; Zhou, Z.; Wegh, R. T.; Welter, R. Highly Luminescent Cu(I) Complexes for Light-emitting Electrochemical Cells *Adv. Mater.* **2006**, *18*, 1313-1316.

[10] Zhang, Q.; Zhou, Q.; Cheng, Y.; Wang, L.; Ma, D.; Jing, X.; Wang, F. Highly Efficient Electroluminescence from Green-light-emitting Electrochemical Cells Based on Cu^{I} Complexes *Adv. Funct. Mater.* **2006**, *16*, 1203-1208.

[11] Moudam, O.; Kaeser, A.; Delavaux-Nicot, B.; Duhayon, C.; Holler, M.; Accorsi, G.; Armaroli, N.; Séguy, I.; Navarro, J.; Destruel, P.; Nierengarten, J.-F. Electrophosphorescent Homo- and Heteroleptic Copper(I) Complexes Prepared from Various Bisphosphine Ligands *Chem. Commun.* **2007**, 3077-3079.

[12] Costa, R. D.; Tordera, D.; Ortí. E.; Bolink, H. J.; Schönle, J.; Graber, S.; Housecroft, C. E.; Constable, E. C.; Zampese, J. A. Copper(I) Complexes for Sustainable Light-emitting Electrochemical Cells *J. Mater. Chem.* **2011**, *21*, 16108-16118.

[13] Asil, D.; Foster, J. A.; Patra, A.; de Hatten, X.; del Barrio, J.; Scherman, O. A.; Nitschke, J. R.; Friend, R. H. Temperature- and Voltage-induced Ligand Rearrangement of a Dynamic Electroluminescent Metallopolymer *Angew. Chem. Int. Ed.* **2014**, *53*, 8388-8391.

[14] Bizzarri, C.; Strabler, C.; Prock, J.; Trettenbrein, B.; Ruggenthaler, M.; Yang, C.-H.; Polo, F.; Lordache, A.; Brüggeller, P.; De Cola, L. Luminescent Dinuclear Cu(I) Complexes Containing Rigid Tetraphosphine Ligands *Inorg. Chem.* **2014**, *53*, 10944-10951.

[15] Keller, S.; Constable, E. C.; Housecroft, C. E.; Neuburger, M.; Prescimone, A.; Longo, G.; Pertegás, Sessolo, M.; Bolink, H. J. $[Cu(bpy)(P\text{^}P)]^{+}$ Containing Light-emitting Electrochemical Cells: Improving Performance through Simple Substitution *Dalton Trans.* **2014**, *43*, 16593-16596.

[16] Cid, J.-J.; Mohanraj, J.; Holler, M.; Monti, F.; Accorsi, G.; Karmazin-Brelot, L.; Nierengarten, I.; Malicka, J. M.; Cocchi, M.; Delavaux-Nicot, B.; Armaroli, N.; Nierengarten, J.-F. Dinuclear Cu(I) Complexes Prepared from 2-diphenylphosphino-6-methylpyridine *Polyhedron*, **2014**, *82*, 158-172.

[17] Keller, S.; Pertegás, A.; Longo, G.; Martínez, L.; Cerdá, J.; Junquera-Hernández, J. M.; Prescimone, A.; Constable, E. C.; Housecroft, C. E.; Ortí, E.; Bolink, H. J. Shine Bright or Live Long: Substituent Effects in $[Cu(N\text{^}N)(P\text{^}P)]^{+}$ Based Light-emitting Electrochemical Cells Where N^N is a 6-substituted 2,2'-bipyridine *J. Mater. Chem. C*, **2016**, DOI: 10.1039/c5tc03725e.

[18] Tao, Y.; Yuan, K.; Xu, P.; Li, H.; Chen, R.; Zheng, C.; Zhang, L.; Huang, W. Thermally Activated Delayed Fluorescence Materials Towards the Breakthrough of Organoelectronics *Adv. Mater.* **2014**, *26*, 7931-7958.

[19] Uoyama, H.; Goushi, K.; Shizu, K.; Nomura, H.; Adachi, C. Highly Efficient Organic Light-emitting Diodes from Delayed Fluorescence *Nature*, **2012**, *492*, 234-238.

[20] Blasse, G.; McMillin, D. R. On the Luminescence of Bis (Triphenylphosphine) Phenanthroline Copper (I) *Chem. Phys. Lett.*, **1980**, *70*, 1-3.

[21] Volz, D.; Wallesch, M.; Fléchon, C.; Danz, M.; Verma, A.; Navarro, J. M.; Zink, D. M.; Bräse, S.; Baumann, T. From Iridium and Platinum to Copper and Carbon: New Avenues for More Sustainability in Organic Light-emitting Diodes *Green Chem.* **2015**, *17*, 1988-2011 and references therein.

[22] Zink, D. M.; Bächle, M.; Baumann, T.; Nieger, M.; Kühn, M.; Wang, C.; Klopper, W.; Monkowius, U.; Hofbeck, T.; Yersin, H.; Bräse, S. Synthesis, Structure, and Characterization of Dinuclear Copper(I) Halide Complexes with P^N Ligands Featuring Exciting Photoluminescence Properties *Inorg. Chem.* **2013**, *52*, 2292-2305.

[23] Zhang, Q.; Zhou, Q.; Cheng, Y.; Wang, L.; Ma, D.; Jing, X.; Wang, F. Highly Efficient Green Phosphorescent Organic Light-emitting Diodes Based on Cu^{I} Complexes *Adv. Mater.* **2004**, *16*, 432-436.

[24] Che, G.; Su, Z.; Li, W.; Chu, B.; Li, M. Highly Efficient and Color-tuning Electrophosphorescent Devices Based on Cu(I) Complex *Appl. Phys. Lett.* **2006**, *89*, 1003511.

[25] Walsh, P. J.; Lundin, N. J.; Gordon, K. C.; Kim, J.-Y.; Lee, C.-H. Spectral Characterization of Electroluminescent Devices Containing Functionalized Dipyrido[3,2-a:2′,3′-c]phenazine Complexes *Optical Mater.*, **2009**, *31*, 1525-1531.

[26] McMillin, D. R.; McNett, K. M. Photoprocesses of Copper Complexes That Bind to DNA *Chem. Rev.* **1998**, *98*, 1201-1219.

[27] Cunningham, C. T.; Moore, J. J.; Cunningham, K. L. H.; Fanwick, P. E.; McMillin, D. R. Structural and Photophysical Studies of $Cu(NN)_2^{+}$ Systems in the Solid State. Emission at Last from Complexes with Simple 1,10-Phenanthroline Ligands *Inorg. Chem.* **2000**, *39*, 3638-3644.

[28] Kaeser, A.; Mohankumar, M.; Mohanraj, J.; Monti, F.; Holler, M.; Cid, J.-J.; Moudam, O.; Nierengarten, I.; Karmazin-Brelot, L.; Duhayon, C.; Delavaux-Nicot, B.; Armaroli, N.; Nierengarten J.-F. Heteroleptic Copper(I) Complexes Prepared from Phenanthroline and Bis-Phosphine Ligands *Inorg. Chem.* **2013**, *52*, 12140-12151.

[29] Krylova, V. A.; Djurovich, P. I.; Whited, M. T.; Thompson, M. E. Synthesis and Characterization of Phosphorescent Three-Coordinate Cu(I)–NHC Complexes *Chem. Commun.*, **2010**, *46*, 6696-6698.

[30] Krylova, V. A.; Djurovich, P. I.; Aronson, J. W.; Haiges, R.; Whited, M. T.; Thompson, M. E. Structural and Photophysical Studies of Phosphorescent Three-Coordinate Copper(I) Complexes Supported by an N-Heterocyclic Carbene Ligand *Organometallics*, **2012**, *31*, 7983-7993.

[31] Krylova, V. A.; Djurovich, P. I.; Conley, B. L.; Haiges, R.; Whited, M. T.; Williams, T. J.; Thompson, M. E. Control of Emission Colour with N-Heterocyclic Carbene (NHC) Ligands in Phosphorescent Three-Coordinate Cu(I) Complexes *Chem. Commun.* **2014**, *50*, 7176-7179.

[32] Leitl, M. J.; Krylova, V. A.; Djurovitch, P. I.; Thompson, M. E.; Yersin, H. Phosphorescence versus Thermally Activated Delayed Fluorescence. Controlling Singlet–Triplet Splitting in Brightly Emitting and Sublimable Cu(I) Compounds *J. Am. Chem. Soc.*, **2014**, *136*, 16032-16038.

[33] Marion, R.; Sguerra, F.; Di Meo, F.; Sauvageot, E.; Lohier, J.-F.; Daniellou, R.; Renaud, J.-L.; Linares, M.; Hamel, M.; Gaillard, S. NHC Copper(I) Complexes Bearing Dipyridylamine Ligands: Synthesis, Structural, and Photoluminescent Studies *Inorg. Chem.*, **2014**, *53*, 9181-9191.

[34] Marion, R.; Sguerra, F.; Di Meo, F.; Sauvageot, E.; Lohier, J.-F.; Daniellou, R.; Renaud, J.-L.; Linares, M.; Hamel, M.; Gaillard, S. Correction to NHC Copper(I) Complexes Bearing Dipyridylamine Ligands: Synthesis, Structural, and Photoluminescent Studies *Inorg. Chem.*, **2016**, *55*, 4068.

[35] Visbal, R.; Gimeno, M. C. N-Heterocyclic Carbene Metal Complexes: Photoluminescence and Applications *Chem. Soc. Rev.*, **2014**, *43*, 3551-3574.

[36] Gaillard, S.; Bantreil, X.; Slawin, A. M. Z.; Nolan, S. P. Synthesis and Characterization of IPr^{Me}-Containing Silver(I), Gold(I) and Gold(III) Complexes *Dalton Trans.*, **2009**, 6967-6971.

[37] Arduengo, III, A. J.; Krafczyk, R.; Schmutzler, R. Imidazolylidenes, Imidazolinylidenes and Imidazolidines *Tetrahedron*, **1999**, *55*, 14523-14534.

[38] Gaillard, S.; Elmkaddem, M. K.; Fischmeister, C.; Thomas, C. M.; Renaud, J.-L. Highly Efficient and Economic Synthesis of New Substituted Amino-Bispyridyl Derivatives via Copper and Palladium Catalysis *Tetrahedron Lett.* **2008**, *49*, 3471-3474.

[39] Swarts, A. J.; Mapolie, S. The Synthesis and Application of Novel Ni(II) *N*-Alkyl Dipyridylaldiminato Complexes as Selective Ethylene Oligomerisation Catalysts *Dalton Trans.* **2014**, *43*, 9892-9900.

[40] Citadelle, C. A.; Le Nouy, E.; Bisaro, F.; Slawin, A. M. Z.; Cazin, C. S. J. Simple and Versatile Synthesis of Copper and Silver *N*-Heterocyclic Carbene Complexes in Water or Organic Solvents *Dalton Trans.* **2010**, *39*, 4489-4491.

[41] Ma, D.; Duan, L.; Wei, Y.; Qiu, Y. Trifluoromethylation of Tetraphenylborate Counterions in Cationic Iridium(III) Complexes: Enhanced Electrochemical Stabilities, Charge-Transport Abilities, and Device Performance *Chem. Eur. J.* **2014**, *20*, 15903-15912.

[42] Nelson, D. J.; Collado, A.; Manzini, S.; Meiries, S.; Slawin, A. M. Z.; Cordes, D. B.; Nolan, S. P. Methoxy-Functionalized *N*-Heterocyclic Carbenes *Organometallics*, **2014**, *33*, 2048-2058.

[43] Nitsch, J.; Lacemon, F.; Lorbach, A.; Eichhorn, A.; Cisnetti, F.; Steffen, A. Cuprophilic Interactions in Highly Luminescent Dicopper(I)–NHC–picolyl Complexes – Fast Phosphorescence or TADF? *Chem. Commun.* **2016**, *52*, 2932-2936.

[44] Dietrich, J.; Thorenz, U.; Förster, C.; Heinze, K. Effects of Sequence, Connectivity, and Counter Ions in New Amide-Linked $Ru(tpy)_2$–Re(bpy) Chromophores on Redox Chemistry and Photophysics *Inorg. Chem.* **2013**, *52*, 1248-1264.

[45] Levell, J. W.; Ruseckas, A.; Henry, J. B.; Wang, Y.; Stretton, A. D.; Mount, A; R.; Galow, T. H.; Samuel, I. D. W. Fluorescence Enhancement by Symmetry Breaking in a Twisted Triphenylene Derivative *J. Phys. Chem. A*, **2010**, *114*, 13291-13295.

[46] Moral, M.; Muccioli, L.; Son, W.-J.; Olivier, Y.; Sancho-García, J. C. Theoretical Rationalization of the Singlet–Triplet Gap in OLEDs Materials: Impact of Charge-Transfer Character *J. Chem. Theory. Comput.* **2015**, *11*, 168-177.

[47] Milián-Medina, B.; Gierschner, J. Computational Design of Low Singlet–Triplet Gap All-Organic Molecules for OLED Application *Org. Electron.* **2012**, *13*, 985-991.

[48] It is worth noting that the use of Tamm-Dancoff approximation has not shown significant differences with respect to the conventional TD-DFT frameworks.

[49] Altal, F.; Gao, J. Long-Term Testing of Polymer Light-Emitting Electrochemical Cells: Reversible Doping and Black Spots *Organic electronics* **2015**, *18*, 1-7.

[50] Meier, S. B.; Hartmann, D.; Tordera, D.; Bolink, H. J.; Winnacker, A.; Sarfert, W. Dynamic Doping and Degradation in Sandwich-Type Light-emitting Electrochemical Cells *Phys. Chem. Chem. Phys.* **2012**, *14*, 10886-10890.

[51] Tamayo, A. B.; Garon, S.; Tissa, S.; Djurovich, P. I.; Tsyba, I. M.; Bau, R.; Thompson, M. E. Cationic Bis-cyclometalated Iridium(III) Diimine Complexes and Their Use in Efficient Blue, Green, and Red Electroluminescent Devices *Inorg. Chem.* **2005**, *44*, 8723-8732.

[52] He, L.; Duan, L.; Qiao, J.; Wang, R.; Wei, P.; Wang, L.; Qiu, Y. Blue-Emitting Cationic Iridium Complexes with 2-(1*H*-Pyrazol-1-yl)pyridine as the Ancillary Ligand for Efficient Light-Emitting Electrochemical Cells *Adv. Funct. Mater.* **2008**, *18*, 2123-2131.

[53] He, L.; Duan, L.; Qiao, J.; Dong, G.; Wang, L.; Qiu, Y. Highly Efficient Blue-Green and White Light-emitting Electrochemical Cells Based on a Cationic Iridium Complex with a Bulky Side Group *Chem. Mater.* **2010**, *22*, 3535-3542.

[54] Yang, C.-H.; Beltran, J.; Lemaur, V.; Cornil, J.; Hartmann, D.; Sarfert, W.; Fröhlich, R.; Bizzarri, C.; De Cola, L. Iridium Metal Complexes Containing N-Heterocyclic Carbene Ligands for Blue-Light-emitting Electrochemical Cells *Inorg. Chem.* **2010**, *49*, 9891-9901.

[55] Mydlak, M.; Bizzarri, C.; Hartmann, D.; Sarfert, W.; Schmid, G.; De, C. L. Positively Charged Iridium(III) Triazole Derivatives as Blue Emitters for Light-emitting Electrochemical Cells *Adv. Funct. Mater.* **2010**, *20*, 1812-1820.

[56] He, L.; Duan, L.; Qiao, J.; Zhang, D.; Wang, L.; Qiu, Y. Enhanced Stability of Blue-Green Light-emitting Electrochemical Cells Based on a Cationic Iridium Complex with 2-(1-Phenyl-1*H*-Pyrazol-3-yl)Pyridine as the Ancillary Ligand *Chem. Commun.* **2011**, *47*, 6467-6469.

[57] Hu, T.; Duan, L.; Qiao, J.; He, L.; Zhang, D.; Wang, R.; Wang, L.; Qiu, Y. Stable Blue-Green Light-emitting Electrochemical Cells Based on a Cationic Iridium Complex with Phenylpyrazole as the Cyclometalated Ligands *Org. Electron.* **2012**, *13*, 1948-1955.

[58] Meier, S. B.; Sarfert, W.; Junquera-Hernández, J.; Delgado, M.; Tordera, D.; Ortí, E.; Bolink, H. J.; Kessler, F.; Scopelliti, R.; Grätzel, M.; Nazeeruddin, M. K.; Baranoff, E. A Deep-Blue Emitting Charged Bis-Cyclometallated Iridium(III) Complex for Light-emitting Electrochemical Cells *J. Mater. Chem. C* **2013**, *1*, 58-68.

[59] Sunesh, C. D.; Mathai, G.; Choe, Y. Green and Blue–Green Light-emitting Electrochemical Cells Based on Cationic Iridium Complexes with 2-(4-Ethyl-2-Pyridyl)-1H-Imidazole Ancillary Ligand *Org. Electron.* **2014**, *15*, 667-674.

[60] Evariste, S.; Sandroni, M.; Rees, T. W.; Roldán-Carmona, C.; Gil-Escrig, L.; Bolink, H. J.; Baranoff, E.; Zysman-Colman, E. Fluorine-Free Blue-Green Emitters for Light-emitting Electrochemical Cells *J. Mater. Chem. C* **2014**, *2*, 5793-5804.

[61] Hasan, K.; Donato, L.; Shen, Y.; Slinker, J. D.; Zysman-Colman, E. Cationic Iridium(III) Complexes Bearing Ancillary 2,5-Dipyridyl(pyrazine) (2,5-dpp) and 2,2′:5′,2″-Terpyridine (2,5-tpy) Ligands: Synthesis, Optoelectronic Characterization and Light-emitting Electrochemical Cells *Dalton Trans.* **2014**, *43*, 13672-13682.

[62] Monti, F.; Baschieri, A.; Gualandi, I.; Serrano-Pérez, J. J.; Junquera-Hernández, J. M.; Tonelli, D.; Mazzanti, A.; Muzzioli, S.; Stagni, S.; Roldan-Carmona, C.; Pertegás, A.; Bolink, H. J.; Ortí, E.; Sambri, L.; Armaroli, N. Iridium(III) Complexes with Phenyl-tetrazoles as Cyclometalating Ligands *Inorg. Chem.* **2014**, *53*, 7709-5084.

[63] Sunesh, C. D.; Shanmugasundaram, K.; Subeesh, M. S.; Chitumalla, R. K.; Jang, J.; Choe, Y. Blue and Blue-Green Light-emitting Cationic Iridium Complexes: Synthesis, Characterization, and Optoelectronic Properties *ACS Appl. Mater. Interfaces* **2015**, *7*, 7741-7721.

[64] Gaussian 09, Revision D.01, Frisch, M. J.; Trucks, G. W.; Schlegel, H. B.; Scuseria, G. E.; Robb, M. A.; Cheeseman, J. R.; Scalmani, G.; Barone, V.; Mennucci, B.; Petersson, G. A.; Nakatsuji, H.; Caricato, M.; Li, X.; Hratchian, H. P.; Izmaylov, A. F.; Bloino, J.; Zheng, G.; Sonnenberg, J. L.; Hada, M.; Ehara, M.; Toyota, K.; Fukuda, R.; Hasegawa, J.; Ishida, M.; Nakajima, T.; Honda, Y.; Kitao, O.; Nakai, H.; Vreven, T.; Montgomery, J. A., Jr.; Peralta, J. E.; Ogliaro, F.; Bearpark, M.; Heyd, J. J.; Brothers, E.; Kudin, K. N.; Staroverov, V. N.; Kobayashi, R.; Normand, J.; Raghavachari, K.; Rendell, A.; Burant, J. C.; Iyengar, S. S.; Tomasi, J.; Cossi, M.; Rega, N.; Millam, N. J.; Klene, M.; Knox, J. E.; Cross, J. B.; Bakken, V.; Adamo, C.; Jaramillo, J.; Gomperts, R.; Stratmann, R. E.; Yazyev, O.; Austin, A. J.; Cammi, R.; Pomelli, C.; Ochterski, J. W.; Martin, R. L.; Morokuma, K.; Zakrzewski, V. G.; Voth, G. A.; Salvador, P.; Dannenberg, J. J.; Dapprich, S.; Daniels, A. D.; Farkas, Ö.; Foresman, J. B.; Ortiz, J. V.; Cioslowski, J.; Fox, D. J. *Gaussian, Inc.*, Wallingford CT, *2009*.

[65] Chai, J. D.; Head-Gordon, M. Systematic Optimization of Long-range Corrected Hybrid Density Functionals *Phys. Chem. Chem. Phys.* **2008**, *10*, 6615-6620.

[66] Chai, J.-D.; Head-Gordon, M. J. *Chem. Phys.* **2008**, *128*, 084106.

[67] Di Meo, F.; Sancho Garcia, J. C.; Dangles, O.; Trouillas, P. Highlights on Anthocyanin Pigmentation and Copigmentation: A Matter of Flavonoid π-Stacking Complexation To Be Described by DFT-D *J. Chem. Theory Comput.* **2012**, *8*, 2034-2043.

[68] Minenkov, Y.; Singstad, Å.; Occhipinti G.; Jensen V. R. The Accuracy of DFT-Optimized Geometries of Functional Transition Metal Compounds: a Validation Study of Catalysts for Olefin Metathesis and

Other Reactions in the Homogeneous Phase *Dalton Trans.* **2012**, *41*, 5526-5541.

[69] Rustioni, L., Di Meo, F., Guillaume, M., Failla, O., Trouillas, P. Tuning Color Variation in Grape Anthocyanins at the Molecular Scale *Food Chem.* **2013**, *141*, 4349-4357.

[70] Humphrey, W.; Dalke, A.; Schulten, K. VMD: Visual Molecular Dynamics *J. Molec. Graphics* **1996**, *14*, 33-38.

Designing NHC-Copper(I) Dipyridylamine Complexes for Blue Light-Emitting Electro-chemical Cells

Margaux Elie,[‡,†] Fabien Sguerra,[‡,∥] Florent Di Meo,[‡,§] Michael D. Weber,[‡,≠] Ronan Marion,[†] Adèle Grimault,[†] Jean-François Lohier,[†] Aurélie Stallivieri,[†] Arnaud Brosseau,[¥] Robert B. Pansu,[¥] Jean-Luc Renaud,[†] Rubén D. Costa,[*,≠] Mathieu Linares,[*,§,#] Matthieu Hamel,[*,∥] Sylvain Gaillard[*,†]

Cheap and Bright: A series of tricoordinated cationic copper(I) complexes bearing various NHC and dpa ligands has been prepared to rationalize the role of both ligands on their photophysical properties. Owing to their excellent blue emitting features, the first blue LECs based on copper(I) complexes are presented.